IEEE Access
Multidisciplinary ⋮ Rapid Review ⋮ Open Access Journal

Received 10 January 2024, accepted 21 January 2024, date of publication 26 January 2024, date of current version 6 February 2024.

Digital Object Identifier 10.1109/ACCESS.2024.3358834

RESEARCH ARTICLE

Design and Implementation of an X-Band Horn Antenna With a Metamaterial Lens Using 3D Printing Technology

JI-HAENG CHO[1], KYOUNG-YOUL PARK[1], CHUL-MIN LIM[1], AND HAE-WON SON[2]

[1]Agency for Defense Development, Daejeon 34186, South Korea
[2]Electronics and Information Engineering, College of Engineering, Jeonbuk National University, Jeonju 54896, South Korea

Corresponding author: Hae-Won Son (hwson@jbnu.ac.kr)

This work was supported by the Agency For Defense Development Grant funded by the Korean Government under Grant UI912884601.

ABSTRACT This paper presents the design and implementation of an X-band horn antenna, which operates over a frequency range of 7 – 9 GHz for small satellite communication systems in Low Earth Orbit (LEO), employing metamaterials and 3D printing technology. It was fabricated using a polymer-based material through a 3D printer and subsequently coated with copper. The horn antenna with a metamaterial lens (meta lens) and septum polarizer is fabricated as a single structure, eliminating the need for additional mechanical structures and parts for assembly of the antenna. This results in a significant reduction in weight compared to a conventional antenna manufactured using traditional methods. To enhance the directivity of the conical horn antenna, the meta lens horn antenna incorporates a periodic lattice-shaped metamaterial. Additionally, a septum polarizer is integrated to achieve circular polarization. The metamaterial lens used in this paper exhibits Near-Zero Refractive Index (NZRI) characteristics within the operating frequency band. It is positioned inside the conical horn antenna to compensate for the field phase difference between the horn's edge and vertex. This compensation leads to a uniform phase distribution across the aperture, resulting in improved antenna directivity. The simulated and measured results show that the meta lens enhances the gain by over 1 dB within the frequency band of interest compared to the conventional horn of the same size. Furthermore, it exhibits a return loss below 20 dB. The proposed antenna was fabricated as a monolithic lightweight structure using the Fused Deposition Modeling (FDM) technique and subsequently metalized through the electro-less plating process. The stability of electrical properties has been verified in a thermal vacuum environment test to ensure its functionality in an LEO environment, characterized by significant temperature fluctuation.

INDEX TERMS 3D printing, electro-less plating, low earth orbit (LEO), metamaterial lens, near zero refractive index (NZRI), satellite communication, X-band horn antenna.

I. INTRODUCTION

The satellite industry has primarily focused on the development of applications in the geostationary orbit, such as communication, surveillance, and reconnaissance operations. However, there is currently a growing trend toward the active utilization of micro and small satellites in Low Earth Orbit (LEO) across various fields, including environmental monitoring, scientific data collection, and wireless relay, among others [1]. There has been a substantial increase in the number of institutions and companies aiming to enter the LEO market. As a result, extensive research and development efforts have been undertaken in the field of LEO communication systems, enabling a relatively low risk of failure and reduced costs [2], [3]. A micro satellite, commonly known as a Micro Sat, refers to a satellite weighing around 100 kg including the communication components. Therefore, it is crucial to reduce the size and weight of Micro Sat

The associate editor coordinating the review of this manuscript and approving it for publication was Giorgio Montisci.

communication components, especially antennas [4]. However, antennas and other RF components manufactured using CNC (Computer Numerical Control) metal milling technology tend to be heavy and large, posing challenges for their integration onto a Micro Sat. Therefore, there is a pressing need for the miniaturization and weight reduction of communication components. To address these challenges, some studies have introduced the utilization of Selective Laser Melting (SLM) 3D printing with metal powder to fabricate antennas and satellite components [5], [6]. And recently, some research groups have applied SLM with metal powder to manufacture horn antenna [7], [8]. However, it is important to note that metal powders are heavier than polymer materials and their surface tend to become rough during the manufacturing process. Other papers demonstrate the manufacturing of horn antennas using polymer-based 3D printers, but these proposed structures have been made in a disassembled form to facilitate plating or manual painting with a conductive layer [9], [10]. Thus, additional mechanical structures and parts are necessary for the assembly of the antenna. In this paper, we designed a meta lens horn antenna and septum polarizer for satellite communication, with a particular emphasis on fabricating these complex configurations as a monolithic lightweight structure and exploring the feasibility of operating it in a low earth orbit space environment.

Metamaterials are materials that are intentionally designed to exhibit artificial properties that are not typically found in nature. These materials are engineered with an appropriate periodic structure, often utilizing resonance structures, often to achieve effective negative permittivity and negative permeability within specific frequency ranges of interest [11], [12]. In the realm of RF components utilizing metamaterials, various studies have been conducted, including investigations on perfect lenses [13], Miniaturization of patch antennas [14], waveguide filtering [15] and leveraging electromagnetic (EM) wave characteristics in metamaterial media. Particularly, there has been extensive research on the feasibility of designing bulk materials with simultaneous permittivity and permeability values close to zero. Several studies have demonstrated that materials with low operational wave numbers (due to a refractive index near zero) exhibit minimal phase variation during propagation [16], [17]. Taking into account the manufacturing convenience across different methods of metamaterial horn antenna fabrication, we introduce an antenna with a meta lens, which utilizes a lattice structure composed of electric wire media to enhance the directivity.

This paper is organized as follows. In Section II, the design of the meta lens horn antenna is presented. Section III describes the manufacturing method of the proposed antenna using 3D printing and metallization. In Section IV, the measured results of the proposed antenna's electrical properties (S-parameter, Gain, Radiation pattern) and the thermal vacuum chamber test are presented. Finally, Section V provides a conclusion of this paper.

II. DESIGN OF META LENS HORN ANTENNA

The proposed antenna is illustrated in Fig. 1. This antenna consists of a conical horn, meta lens, and septum polarizer.

The antenna integrates a meta lens into the conical horn structure, enhancing the antenna's directivity by achieving uniformity in the phase front of the E-field radiated from the horn. The phase front of the E-field radiated from the horn varies based on factors such as the thickness and the dimensions of the electric displacement, D_{air}, of the meta lens. The air region of the meta lens, as depicted in Fig.1, is referred to as D_{air}. Hence, these factors of the meta lens impact the directivity of the horn antenna [18].

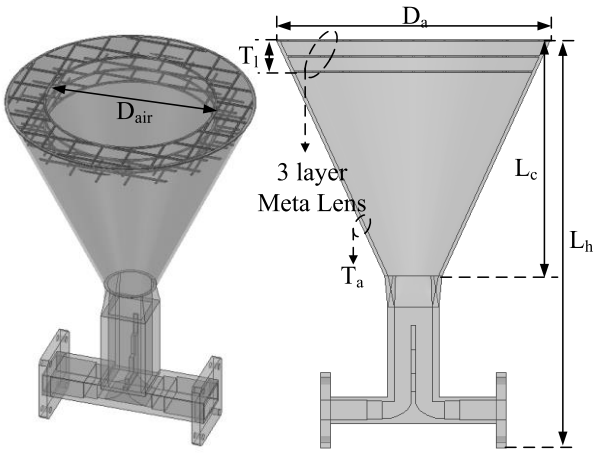

FIGURE 1. Structure of the meta lens horn antenna.

Table 1 provides the design parameters for the proposed NZRI meta lens horn antenna and λ_o represents the free space wavelength at 8 GHz.

TABLE 1. Design parameters of the meta lens horn antenna.

Parameter	Value [mm](λ_o)	Parameter	Value [mm] (λ_o)
L_h	260 (6.93)	L_c	150 (4)
D_a	170 (4.53)	T_a	2 (0.05)
D_{air}	59 (1.57)	T_l	21 (0.56)

A. A PROPERTIES OF NZRI MATERIALS

As a study based on the near-zero refraction of a metamaterial, the radiation beam of a point source inside a slab with a near-zero refractive index material will be refracted in a direction very close to the normal. As a result, all refracted rays converge toward almost the same direction around the normal [19]. This indicates that the NZRI metamaterial lens (meta lens) can be utilized as a superstrate in the aperture of a horn antenna. By doing so, the radiation beams of the antenna can be effectively focused, resulting in enhanced directivity. The NZRI exhibits a refractive index close to zero within the frequency band of interest. The relationship

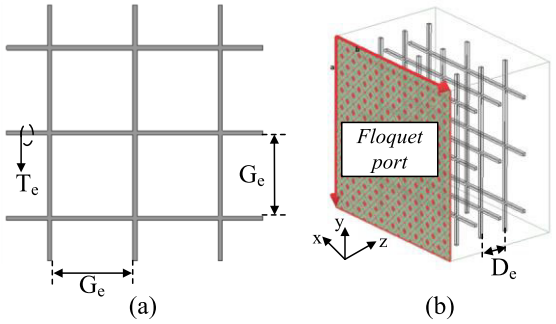

FIGURE 2. The unit cell of the meta lens. (a) Front of view of the unit cell (b) Layout of the unit cell.

TABLE 2. Design Parameters of Unit cell of proposed NZRI meta lens.

Parameter	Value [mm]
Thickness of Electric rod(T_e)	1
Gap of Electric rod(G_e)	19
Distance of Electric rod(D_e)	9

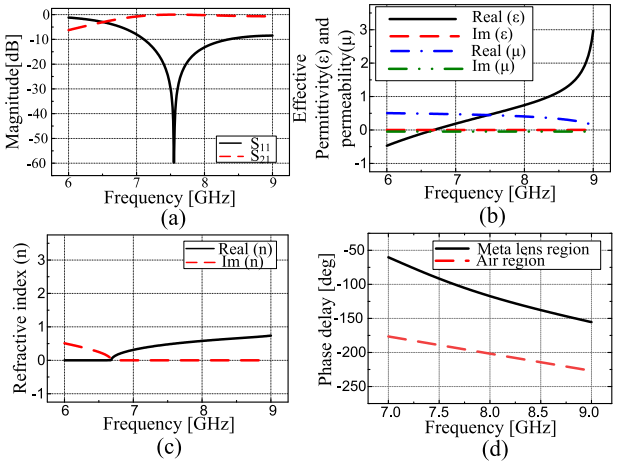

FIGURE 3. Simulated S-parameter for the unit cell and electromagnetic properties retrieved from S-parameter. (a) S11 and S21 of unit cell. (b) Retrieved effective permittivity and permeability. (c) Retrieved effective refractive index. (d) Phase delay change with frequency of the meta lens unit cell.

between the refractive index and the constitutive parameters (relative permittivity (ε_r), and relative permeability (μ_r)) is expressed by

$$n = \pm\sqrt{\varepsilon_r \mu_r} \tag{1}$$

The effective relative permittivity of a media is described with the plasma resonant frequency as shown in (2).

$$\varepsilon_p = 1 - \frac{\omega_p^2}{\omega^2} \tag{2}$$

where ω_p is the plasma resonant frequency and ω denotes the frequency of the propagating electromagnetic wave. Meanwhile, the wavenumber (k) and phase velocity (V_p) of the electromagnetic wave through a media are described by

$$k = \omega\sqrt{\mu\epsilon} \tag{3}$$

$$V_p = \frac{\omega}{k} \tag{4}$$

where the constitutive parameters are relative permittivity (ε), and permeability (μ). In the operating frequency range, when the permittivity and permeability of the metamaterial are smaller than '1' and close to '0', the wavenumber (k) approaches zero, leading to an increase in phase velocity (V_p) [20]. As a result, the propagation of a low wavenumber in a metamaterial, which occurs just above the plasma frequency, exhibits relatively minimal phase variation. These characteristics can be used for the horn antenna application to achieve a uniform phase distribution across the aperture, thereby enhancing the antenna's directivity. The meta lens used in this paper is similar to the one illustrated by Wu et al. [21]. The configuration of the unit cell for the meta lens is presented in Fig. 2. The Unit cell is constructed in the form of a lattice structure using electric rods and consists of three layers to create a meta lens. The S-parameter of the unit cell was extracted using the Ansys HFSS EM tool. To simulate the periodic structure, Floquet port and primary-secondary boundary conditions have been used [22], [23].

The design parameters for the unit cell, as shown in Fig.2, are summarized in Table 2. The resonant frequency of the meta lens unit cell is primarily influenced by G_e and D_e.

By adjusting the design variables, the resonant frequency of the unit cell can be modified, allowing it to be designed with a refractive index close to '0' within the desired frequency range.

Fig. 3(a) presents the simulated results of S-parameters for the unit cell and the effective constitutive parameters (permittivity, permeability, refractive index), which are shown in Fig. 3(b) to Fig. 3(c). The effective constitutive parameters can be calculated using the retrieval method proposed in the [24], [25]. The unit cell exhibits good impedance matching with free space within the operating frequency range and demonstrates resonance properties at 7.55 GHz. The electromagnetic properties of the unit cell are depicted in Fig. 3(b) to Fig. 3(c). The real part of the effective permittivity ranges from 0.3 to 1, the effective permeability varies from 0.5 to 0.4 and the refractive index falls between 0.4 to 0.6 within the frequency range of interest. Fig. 3(d) shows the phase delay change with frequency of the meta lens as designed in this paper compared to that of the air. The phase velocity in the meta lens region is higher, and this characteristic can be exploited to compensate for the phase difference occurring at the edge of the horn antenna aperture.

B. OPTIMIZATION OF GAIN FOR CONICAL HORN ANTENNA WITH META LENS

A conical horn antenna is designed in the form of a truncated cone and is connected to a circular waveguide. The

radiation characteristics of the antenna are determined by the magnitude and phase distributions of electromagnetic waves on its aperture [26]. The shape of the conical horn antenna is depicted in Fig. 4, with a length of 150 mm, chosen considering its integration onto the Small Sat. Referring to Fig. 4(a), when the electromagnetic source radiates from the virtual vertex inside the horn antenna, the phase across the aperture varies, leading to a phase difference of 'Δs' between the aperture phases. As a result, the E-field propagates in a spherical wave, not a plane wave. The phase difference increases with a larger aperture diameter. For a conical horn antenna with a fixed length 'L_c', if the aperture diameter exceeds the optimal value, then the directivity of the antenna decreases due to the significant phase variation at the aperture [27].

Fig. 4(b) presents the simulated results of the conical horn antenna's directivity as the aperture diameter varies from $D_c = 90$ mm to 190 mm in increments of 20 mm, with the conical length fixed at $L_c = 150$ mm. It can be observed that the directivity of the conical horn antenna starts to decrease once the aperture diameter exceeds 150 mm.

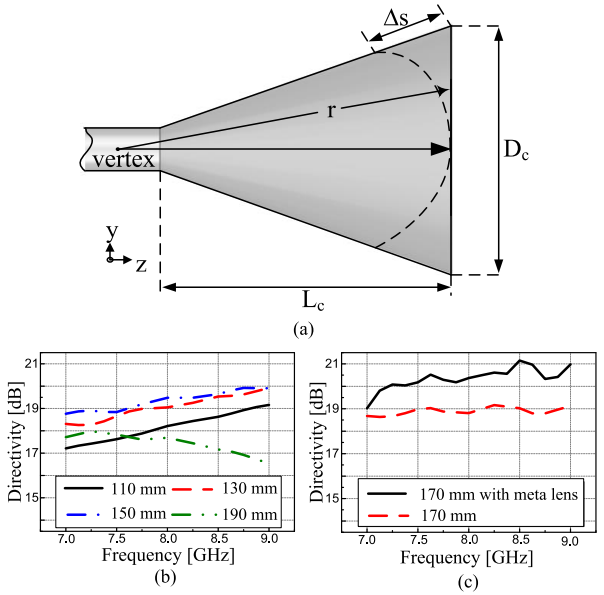

FIGURE 4. (a) Geometry of conical horn. (b) Directivity of conical horn depends on aperture size (c) Directivity of conical horn with 170 mm aperture size depends on with and without meta lens.

In this paper, the aperture diameter is fixed at 170 mm and the meta lens is employed to enhance the directivity of the horn antenna by compensating the phase difference Δs. The aperture diameter size for integrating the meta lens is due to the fact that the compensatory effect for phase differences is not significant when a meta lens is inserted into a 150 mm horn aperture. The simulation results demonstrate that incorporating the meta lens on the conical horn antenna led to an increase in the directivity by over 1 dB more within the frequency range of interest compared to the horn antenna with the same aperture size of 170 mm.

Fig. 5 illustrates the distribution of the E-field magnitude around the horn antenna at f = 7.8 GHz. The phase front of the E-field radiated from the horn antenna propagates in a spherical wave front. However, when the meta lens is inserted into the aperture, the phase front of the E-field radiated from the horn antenna propagates as a quasi-plane wave, as depicted in Fig. 5.

Therefore, by utilizing the meta lens, the phase difference in the E-field that occurs due to the large aperture size can be effectively compensated. This compensation leads to an improvement in the directivity of the horn antenna and an increase in antenna gain.

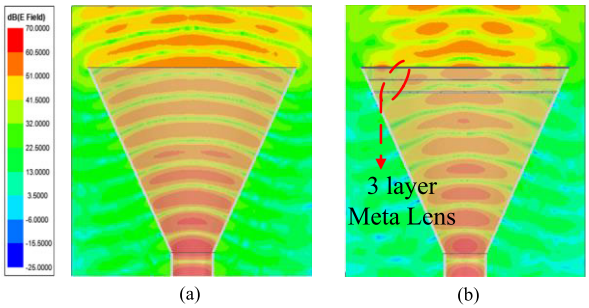

FIGURE 5. The simulated results of the E-field distribution around the horn antenna at 7.8 GHz (a) without the meta lens and (b) with the meta lens.

C. SEPTUM POLARIZER

The septum polarizer consists of a stepped waveguide with two WR-112 input terminals, four stepped septums, and a square-to-circular waveguide transition, as illustrated in Fig. 6.

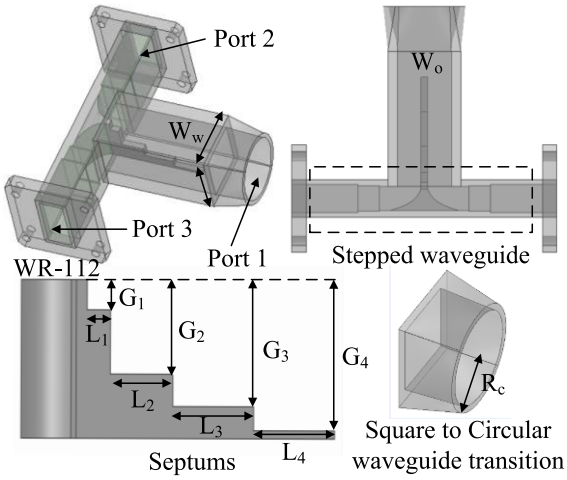

FIGURE 6. Structure of septum polarizer.

This septum polarizer has a staircase-shaped partition wall (septum) located at the center of the square waveguide, dividing it into two rectangular ports. It serves the purpose of converting transmitted EM waves with orthogonal linear polarization into EM waves with orthogonal circular polarization and vice versa in received EM waves with orthogonal

circular polarization [28]. Meanwhile, the stepped waveguide serves the purpose of impedance matching to the WR-112 input terminal, while the square-to-circular waveguide transition is designed to facilitate mode conversion and impedance matching with a conical horn.

D. SIMULATION RESULTS

The simulated results of return loss and the isolation of the conical horn antenna, both with and without the meta lens, are shown in Fig. 7. The meta lens horn antenna exhibits slightly degraded characteristics in terms of return loss and isolation compared to the horn antenna without the meta lens. However, the return loss remains above 20 dB, indicating satisfactory performance.

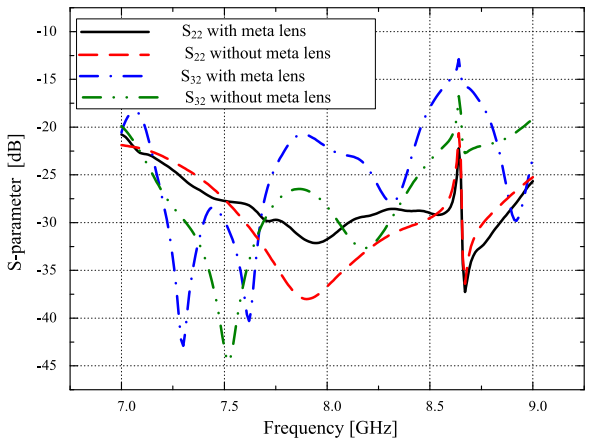

FIGURE 7. The simulated S-parameters of the horn antenna with and without the meta lens.

The simulated results of the gain and axial ratio for the conical horn antenna, both with and without meta lens, are shown in Fig. 8.

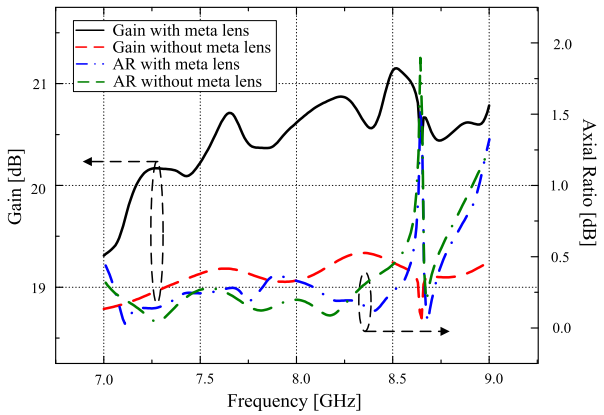

FIGURE 8. Simulated results on Gain and Axial Ratio of the horn antenna with and without the meta lens.

The simulation results show that incorporating the meta lens into the conical horn antenna increases the antenna gain by more than 1 dB in the frequency band of interest. Additionally, the axial ratio (AR) remains below 0.5 dB.

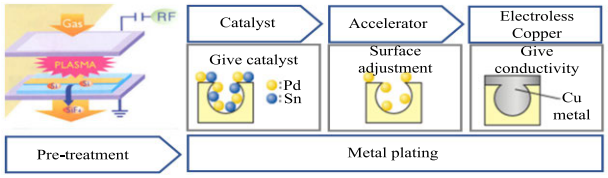

FIGURE 9. The metal coating process (electro-less plating).

III. IMPLEMENTATION OF META LENS HORN ANTENNA; 3D PRINTING AND METAL COATING

When producing the meta lens horn antenna through conventional CNC processing, the conical horn, meta lens, and septum polarizer need to be fabricated individually and then assembled. This requirement leads to the utilization of mechanical structure and parts for connecting the antenna elements, leading to an increase in the overall weight. Alternatively, the soldering technique for creating a meta material from copper wire may vary depending on the level of production maturity [29], [30]. Therefore, creating an integral structure by inserting the lattice-shaped meta lens into the horn aperture, as presented in this paper, using a typical processing method is challenging. Additionally, the weights of materials used for antenna fabrication are crucial when considering the high cost per gram of reaching LEO. For this device, copper generally weighs 8.96 g/cm^3, while Poly-Ether-Ketone-Ketone (PEKK) weighs 1.3 g/cm^3. Hence, in this paper, we employed 3D printing and metal coating methods to reduce the weight of the antenna. By designing the antenna as a monolithic structure, we eliminate the need for mechanical parts between components, which significantly reduces the weight.

The meta lens horn antenna was fabricated using the Fused Deposition Modeling (FDM) method with a Stratasys Fortus 450mc 3D printer and the material used for fabrication was PEKK. This 3D printer possesses a layer resolution ranging from 330 to 127 um [31].

Meanwhile, the LEO environment is characterized by low pressure ($10^{-6} \sim 10^{-7}$ torr) due to high vacuum and experiences extreme temperature variation depending on its position relative to the sun. It is also influenced by various types of radiation energy. Poly materials exposed to such an environment can undergo decomposition, leading to the release of a certain amount of gas, in a phenomenon known as outgassing. This outgassing can adversely affect electronic components, including RF components, and potentially lead to malfunctions. Therefore, it is crucial to select materials that can withstand the temperature variations and vacuum conditions of the LEO environment.

PEKK is a representative high-performance polymer material known for its excellent mechanical strength and heat resistance, making it widely used in the aerospace field.

The meta lens horn has a semi-enclosed structure, which makes it challenging to apply conventional metal coating

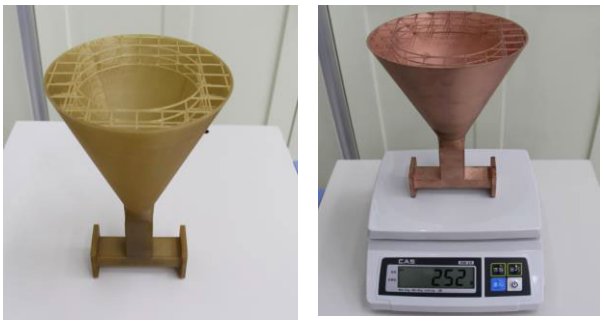

(a) (b)

FIGURE 10. The prototype of the meta lens antenna (a) pre-metalizing (b) post-metalizing.

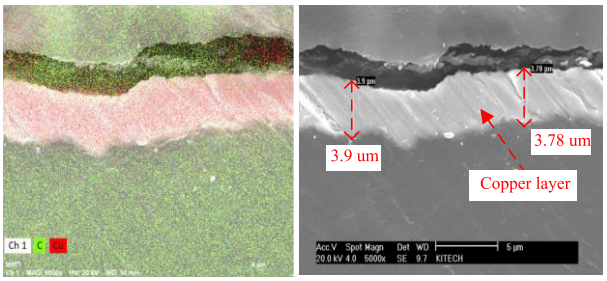

(a) (b)

FIGURE 11. Microscopic view (a) Electron Probe Micro Analysis mapping (b) measured copper layer thickness.

methods to the interior of the horn antenna. Furthermore, the material options for coating with electroplating are limited. Therefore, electro-less plating was utilized to coat the meta lens horn antenna with copper.

Fig. 9 illustrates the electro-less plating process. In the pre-treatment stage, foreign substances within the non-conductive section of the inner wall to be plated are removed.

Simultaneously, a conditioning agent is applied to facilitate the effective absorption of palladium during the subsequent palladium catalyst phase. Following this, the catalyst and accelerator phase involves the adsorption of palladium onto the inner wall. Finally, during the electro-less plating stage, a chemical copper plating process takes place, enhancing the electrical properties through an oxidation-reduction reaction involving the palladium adsorbed onto the non-conductive portion of the inner wall.

Fig. 10 presents the pre- and post-metal coating images of the meta lens horn antenna. The antenna is fabricated as a monolithic structure using a 3D printer, eliminating the need for assembling separate components. As a result, the weight of the prototype antenna is merely 252 g.

Fig. 11 shows the results of measuring the thickness of the metal coating on the surface using electron microscope after applying the metal coating to the meta lens horn antenna. Through high-resolution imaging magnified by 5000 times, the copper layer's thickness is observed to be in the range of

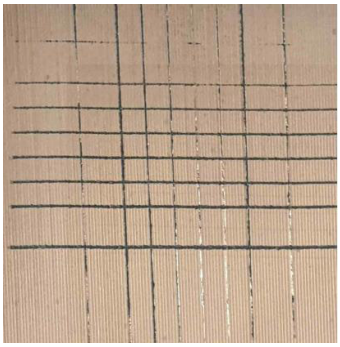

FIGURE 12. The test result of the electro-less plating adhesive strength.

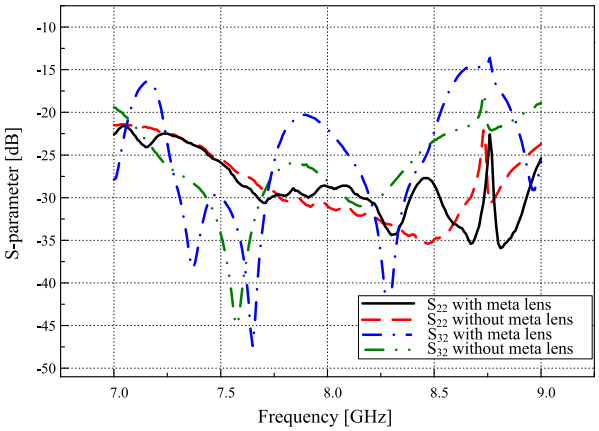

FIGURE 13. The measured results of the return loss and isolation of the horn antenna with and without the meta lens.

3.78 to 3.9 um. The images affirm that a sufficiently thick copper layer has been successfully applied to the meta lens horn antenna, particularly considering the skin depth of the copper in the X band.

The adhesive strength of electro-less plating was assessed using the measurement method specified in ASTM D3359-17 [32]. The specimen's surface, as shown in Fig. 12, was incised using a sharp blade, and an adhesion test was performed with a tape possessing an adhesive strength of 6.56 N/cm. The test results revealed a commendable adhesive strength falling within the 4B to 5B range, in accordance with the adhesion test result classification outlined in the ASTM standards.

IV. MEASUREMENT RESULTS

We produced two horn antennas, with and without the meta lens, to validate the gain enhancement attributed to the meta lens. The electrical performance metrics of the horn antenna, with and without the meta lens, were measured in an anechoic chamber.

The measured results of the return loss and isolation of the conical horn antenna, both with and without the meta lens, are shown in Fig. 13. The meta lens horn antenna exhibits slightly degraded characteristics in terms of return loss and

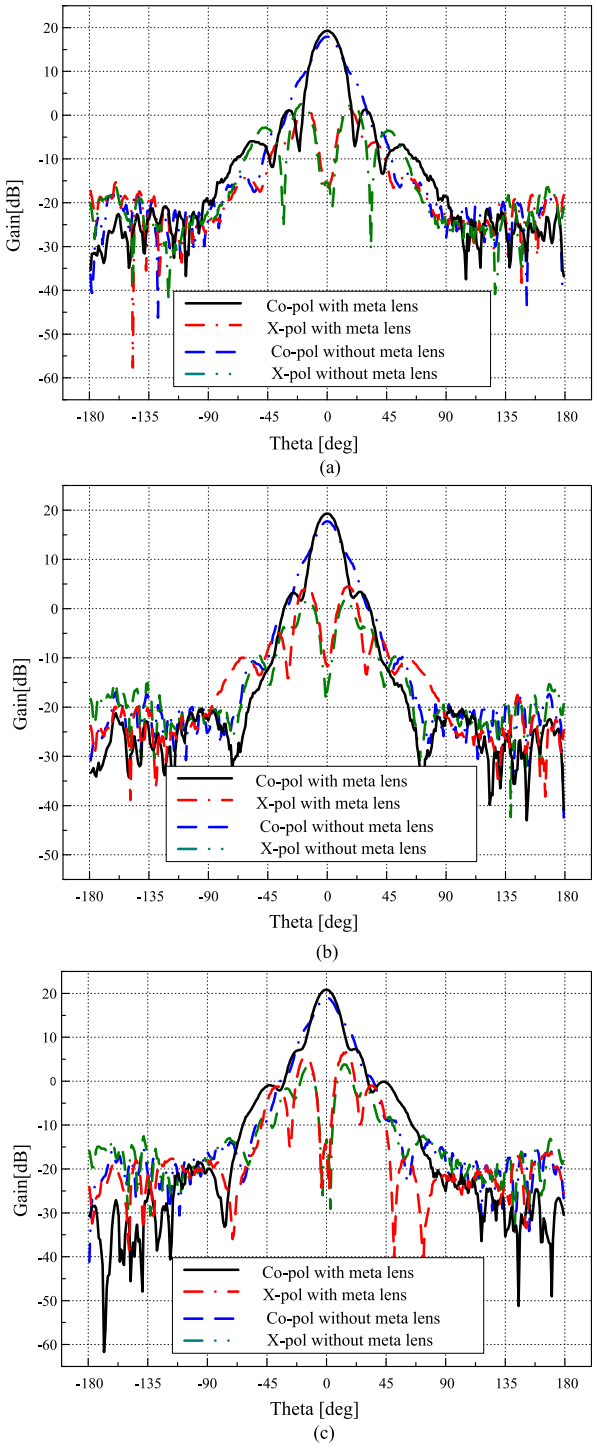

FIGURE 14. The measured radiation pattern of the horn antenna with and without the meta lens (a) at 7.3 GHz (b) at 7.8 GHz (c) at 8.3 GHz.

isolation compared to the horn antenna without the meta lens. However, the return loss and isolation remain above 20 dB within the frequency range of interest, indicating satisfactory performance.

Fig. 14 depicts the measured radiation pattern of the horn antenna with and without the meta lens. The radiation pattern of the meta lens horn antenna exhibits a narrower beam width and increased gain in comparison to the horn antenna without the meta lens.

The measured results of the gain and axial ratio of the conical horn antenna, both with and without meta lens are shown in Fig. 15.

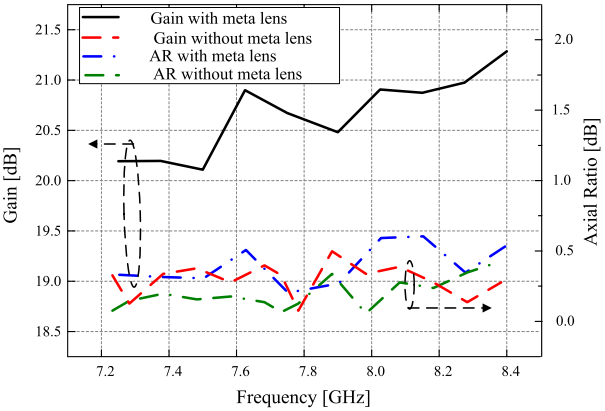

FIGURE 15. Measured results on Gain and Axial Ratio of horn antenna with and without meta lens.

The results demonstrate that the meta lens horn antenna exhibits a gain increase of 1dB or more within the frequency range of interest, which is consistent with the simulation findings.

Fig. 16 presents the thermal vacuum chamber used in the experiment to evaluate the meta lens horn antenna's performance in LEO environments.

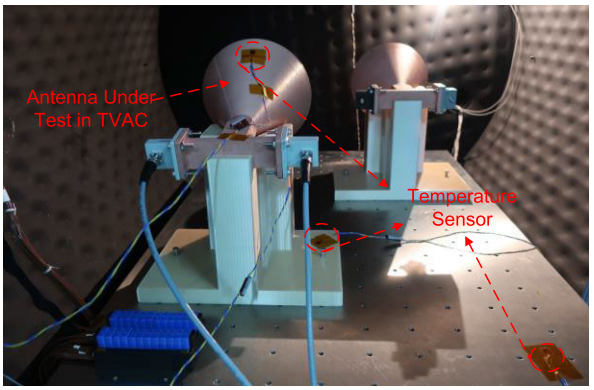

FIGURE 16. The measurement setup of the thermal vacuum test.

Multiple temperature sensors were installed to measure the temperature variations within the chamber and on the meta lens horn antenna. The meta lens horn antenna underwent thorough testing within this chamber. The thermal vacuum conditions were characterized as follows: (the temperature range varied from -50 °C to 70 °C, while the vacuum level ranged from 10^{-4} to 10^{-5} torr). As a result of visual and mechanical inspection, no changes were observed in terms of the shape, quality deterioration of the metal coating, and the electrical properties of the meta lens horn antenna following the thermal vacuum test.

V. CONCLUSION

This paper presents the design and implementation of an X-band horn antenna with a meta lens using 3D printing technology. The incorporation of the meta lens in the horn antenna design has been utilized to enhance its directivity, resulting in a shorter antenna length. Furthermore, in order to reduce weight, the proposed horn antenna was fabricated using a PEKK material with a 3D printer and subsequently coated with copper. The manufacturing process employed FDM with PEKK, a material with high thermal resistance. By employing 3D printing and metal coating in the manufacturing process of the meta lens horn antenna, it becomes possible to achieve a weight reduction of approximately 1/7 compared to the conventional manufacturing method, taking into account solely the material proportion, without considering the weight of fasteners for assembly. The simulated and measured results demonstrate that the meta lens horn antenna exhibits a gain increase of 1 dB or more compared to the horn antenna without the meta lens in the frequency range of interest. Lastly, the electrical and physical characteristics of the proposed horn antenna were verified through a thermal vacuum test to confirm its operability in LEO environments.

REFERENCES

[1] S. Gao, K. Clark, M. Unwin, J. Zackrisson, W. A. Shiroma, J. M. Akagi, K. Maynard, P. Garner, L. Boccia, G. Amendola, G. Massa, C. Underwood, M. Brenchley, M. Pointer, and M. N. Sweeting, "Antennas for modern small satellites," *IEEE Antennas Propag. Mag.*, vol. 51, no. 4, pp. 40–56, Aug. 2009, doi: 10.1109/MAP.2009.5338683.

[2] A. K. Nervold, J. Berk, J. Straub, and D. Whalen, "A pathway to small satellite market growth," *Adv. Aerosp. Sci. Technol.*, vol. 1, no. 1, pp. 14–20, 2016.

[3] P. Kim, J.-G. Ryu, and W. Byun, "Research trends in global wireless communication technology based on the LEO satellite communication network," *Electron. Telecommun. Trends*, vol. 35, no. 5, pp. 83–91, 2020.

[4] S. Lee and J. Oh, "Development trends of small satellites and military applications," *J. Adv. Navig. Tehnol.*, vol. 21, no. 3, pp. 213–219, Jun. 2017.

[5] B. Zhang, Z. Zhan, Y. Cao, H. Gulan, P. Linnér, J. Sun, T. Zwick, and H. Zirath, "Metallic 3-D printed antennas for millimeter- and submillimeter wave applications," *IEEE Trans. THz Sci. Technol.*, vol. 6, no. 4, pp. 592–600, Jul. 2016.

[6] B. Zhang, R. Li, L. Wu, H. Sun, and Y.-X. Guo, "A highly integrated 3-D printed metallic K-band passive front end as the unit cell in a large array for satellite communication," *IEEE Antennas Wireless Propag. Lett.*, vol. 17, no. 11, pp. 2046–2050, Nov. 2018.

[7] K. Lu, K. W. Leung, and N. Yang, "3-D-printed circularly polarized twisted-ridge horn antenna," *IEEE Trans. Antennas Propag.*, vol. 69, no. 3, pp. 1746–1750, Mar. 2021, doi: 10.1109/TAP.2020.3031764.

[8] Y. Cheng and Y. Dong, "High-gain all-metal 3-D printed lens–horn antenna for millimeter-wave applications," *IEEE Antennas Wireless Propag. Lett.*, vol. 22, pp. 308–312, 2023, doi: 10.1109/LAWP.2022.3209788.

[9] J. S. Chieh, B. Dick, S. Loui, and J. D. Rockway, "Development of a Ku-band corrugated conical horn using 3-D print technology," *IEEE Antennas Wireless Propag. Lett.*, vol. 13, pp. 201–204, 2014, doi: 10.1109/LAWP.2014.2301169.

[10] J. Tak, D. Kang, and J. Choi, "A lightweight waveguide horn antenna made via 3D printing and conductive spray coating," *Microw. Opt. Technol. Lett.*, vol. 59, no. 3, pp. 727–729, Mar. 2017, doi: 10.1002/mop.30374.

[11] D. R. Smith, J. B. Pendry, and M. C. K. Wiltshire, "Metamaterials and negative refractive index," *Science*, vol. 305, no. 5685, pp. 788–792, 2004.

[12] J. Li and C. T. Chan, "Double-negative acoustic metamaterial," *Phys. Rev. E, Stat. Phys. Plasmas Fluids Relat. Interdiscip. Top.*, vol. 70, no. 5, Nov. 2004, Art. no. 055602.

[13] J. B. Pendry, "Negative refraction makes a perfect lens," *Phys. Rev. Lett.*, vol. 85, no. 18, pp. 3966–3969, Oct. 2000.

[14] D. T. Phan, H. L. Phan, and T. Q. H. Nguyen, "A miniaturization of microstrip antenna using negative permittivity metamaterial based on CSRR loaded ground for WLAN applications," *J. Sci. Technol.* vol. 54, no. 6, pp. 689–697, 2016.

[15] Z. Y. Pang, X. Y. Ma, G. Zhao, J. J. Liang, G. L. Huang, and L. Zhao, "A 3D printed filtering waveguide with simple metamaterial construction," *Appl. Comput. Electromagn. Soc. J.*, vol. 2020, pp. 539–544, May 2020.

[16] A. Alu, M. G. Silveirinha, A. Salandrino, and N. Engheta, "Epsilon-near-zero metamaterials and electromagnetic sources: Tailoring the radiation phase pattern," *Phys. Rev. B, Condens. Matter*, vol. 75, no. 15, Apr. 2007, Art. no. 155410.

[17] Y. He, N. Ding, L. Zhang, W. Zhang, and B. Du, "Short-length and high-aperture-efficiency horn antenna using low-loss bulk anisotropic metamaterial," *IEEE Antennas Wireless Propag. Lett.*, vol. 14, pp. 1642–1645, 2015.

[18] D. Ramaccia, F. Scattone, F. Bilotti, and A. Toscano, "Broadband compact horn antennas by using EPS-ENZ metamaterial lens," *IEEE Trans. Antennas Propag.*, vol. 61, no. 6, pp. 2929–2937, Jun. 2013.

[19] S. Enoch, G. Tayeb, P. Sabouroux, N. Guérin, and P. Vincent, "A metamaterial for directive emission," *Phys. Rev. Lett.*, vol. 89, no. 21, Nov. 2002, Art. no. 213902.

[20] J. Canet-Ferrer, "Metamataerials and metasurfaces," in *Metamaterials in Application to Improve Antenna Parameters*. Rijeka, Croatia: InTechOpen, Jan. 2019. [Online]. Available: https://www.intechopen.com/books/6849

[21] Q. Wu, P. Pan, F.-Y. Meng, L.-W. Li, and J. Wu, "A novel flat lens horn antenna designed based on zero refraction principle of metamaterials," *Appl. Phys. A, Solids Surf.*, vol. 87, no. 2, pp. 151–156, Mar. 2007.

[22] A. B. Numan and M. S. Sharawi, "Extraction of material parameters for metamaterials using a full-wave simulator [education column]," *IEEE Antennas Propag. Mag.*, vol. 55, no. 5, pp. 202–211, Oct. 2013.

[23] *Getting Started With HFSS: Floquet Ports*, HFSS, 2021.

[24] X. Chen, T. M. Grzegorczyk, B.-I. Wu, J. Pacheco, and J. A. Kong, "Robust method to retrieve the constitutive effective parameters of metamaterials," *Phys. Rev. E, Stat. Phys. Plasmas Fluids Relat. Interdiscip. Top.*, vol. 70, no. 1, Jul. 2004, Art. no. 016608.

[25] D. R. Smith, D. C. Vier, T. Koschny, and C. M. Soukoulis, "Electromagnetic parameter retrieval from inhomogeneous metamaterials," *Phys. Rev. E, Stat. Phys. Plasmas Fluids Relat. Interdiscip. Top.*, vol. 71, no. 3, Mar. 2005, Art. no. 036617.

[26] C. A. Balanis, *Antenna Theory: Analysis and Design*, 3rd ed. Hoboken, NJ, USA: Wiley, 2005.

[27] N. A. Aboserwal, C. A. Balanis, and C. R. Birtcher, "Conical horn: Gain and amplitude patterns," *IEEE Trans. Antennas Propag.*, vol. 61, no. 7, pp. 3427–3433, Jul. 2013.

[28] F. F. Dubrovka, S. I. Piltyay, R. R. Dubrovka, M. M. Lytvyn, and S. M. Lytvyn, "Optimal designs of X-band waveguide stepped-thickness septum polarizer," *Radioelectron. Commun. Syst.*, vol. 64, no. 9, pp. 494–500, Sep. 2021.

[29] D. Ramaccia, M. Barbuto, A. Monti, A. Verrengia, F. Trotta, D. Muha, S. Hrabar, F. Bilotti, and A. Toscano, "Exploiting intrinsic dispersion of metamaterials for designing broadband aperture antennas: Theory and experimental verification," *IEEE Trans. Antennas Propag.*, vol. 64, no. 3, pp. 1141–1146, Mar. 2016.

[30] C. P. Scarborough, Q. Wu, D. H. Werner, E. Lier, R. K. Shaw, and B. G. Martin, "Demonstration of an octave-bandwidth negligible-loss metamaterial horn antenna for satellite applications," *IEEE Trans. Antennas Propag.*, vol. 61, no. 3, pp. 1081–1088, Mar. 2013, doi: 10.1109/TAP.2012.2227660.

[31] *Stratasys Fortus 450mc*. Accessed: Dec. 2023. [Online]. Available: https://www.stratasys.com/en/3d-printers/printer-catalog/fdm-printers/fortus-450mc/

[32] *ASTM D3359017*. Accessed: Dec. 2023. [Online]. Available: https://webstore.ansi.org/standards/astm/astmd335917

JI-HAENG CHO received the B.S. degree in radio wave engineering from Hanbat National University, Daejeon, South Korea, in 2010, and the M.S. degree in electronics engineering from Jeonbuk National University, Jeonju, South Korea, in 2012, where he is currently pursuing the Ph.D. degree in electronics engineering.

He joined the Agency for Defense Development, Daejeon, in 2012, as a Research Engineer, where he has been a Senior Researcher, since 2019. His research interests include the satellite communication components, such as horn antenna and waveguide filter and phased array antenna systems.

KYOUNG-YOUL PARK received the B.S. and M.S. degrees in radio science and engineering from Kwangwoon University, Seoul, Republic of Korea, in 1999 and 2001, respectively, and the Ph.D. degree in electrical engineering from Michigan State University, East Lansing, MI, USA, in 2013.

He joined the Agency for Defense Development, Daejeon, Republic of Korea, as a Researcher, where he has been the Principal Researcher, since 2001. He has been the Team Leader and the Program Manager of several defense satellite communication development programs for the Korean armed forces. His current research interests include millimeter-wave/terahertz technologies and systems, satellite communication payloads, III–V devices, and RF metamaterials.

CHUL-MIN LIM received the B.S. and M.S. degrees in electric communications engineering from Hanyang University, Seoul, Republic of Korea, in 1986 and 1988, respectively.

He joined the Agency for Defense Development, Daejeon, Republic of Korea, in 1988, as a Research Engineer, where he has been the Principal Researcher, since 2006. He has been a Team Member, the Leader, and the Program Manager of several defense satellite communication systems development programs for the Korean armed forces. His current research interests include RF part fabrication using polymer 3D printing and metalization for space applications, high altitude long endurance (HALE), and high altitude pseudo satellite (HAPS) based communications systems.

HAE-WON SON received the B.S. degree in electronics engineering from Kyungpook National University, Daegu, South Korea, in 1994, and the M.S. and Ph.D. degrees in electrical engineering from the Korea Advanced Institute of Science and Technology (KAIST), Daejeon, South Korea, in 1996 and 2001, respectively. From 1996 to 2003, he was with Samsung Electronics, Suwon, South Korea. From 2003 to 2007, he was with the Electronics and Telecommunications Research Institute (ETRI), Daejeon. In 2007, he joined as the Faculty with Jeonbuk National University, Jeonju, South Korea, where he is currently a Full Professor. His research interests include antennas and propagation, RF/microwave circuits, and RFID/ubiquitous sensor networks.